



LAWRENCE
LIVERMORE
NATIONAL
LABORATORY

Capture and Control of Laser-Accelerated Proton Beams: Experiment and Simulation

F. Nurnberg, I. Alber, K. Harres, M. Schollmeier, M. Roth, W. Barth, H. Eickhoff, I. Hofmann, A. Friedman, D.P. Grote, B. G. Logan

July 14, 2009

PAC 2009
Vancouver, Canada
May 4, 2009 through May 8, 2009

Disclaimer

This document was prepared as an account of work sponsored by an agency of the United States government. Neither the United States government nor Lawrence Livermore National Security, LLC, nor any of their employees makes any warranty, expressed or implied, or assumes any legal liability or responsibility for the accuracy, completeness, or usefulness of any information, apparatus, product, or process disclosed, or represents that its use would not infringe privately owned rights. Reference herein to any specific commercial product, process, or service by trade name, trademark, manufacturer, or otherwise does not necessarily constitute or imply its endorsement, recommendation, or favoring by the United States government or Lawrence Livermore National Security, LLC. The views and opinions of authors expressed herein do not necessarily state or reflect those of the United States government or Lawrence Livermore National Security, LLC, and shall not be used for advertising or product endorsement purposes.

CAPTURE AND CONTROL OF LASER-ACCELERATED PROTON BEAMS: EXPERIMENT AND SIMULATION

F. Nürnberg*, I. Alber, K. Harres, M. Schollmeier, M. Roth, TU Darmstadt, Germany
 W. Barth, H. Eickhoff, I. Hofmann, GSI, Darmstadt, Germany
 A. Friedman, D.P. Grote, B.G. Logan, LBNL/LLNL, Berkeley/Livermore CA, USA

Abstract

This paper summarizes the ongoing studies on the possibilities for transport and RF capture of laser-accelerated proton beams in conventional accelerator structures. First results on the capture of laser-accelerated proton beams are presented, supported by Trace3D, CST particle studio and Warp simulations. Based on these results, the development of the pulsed high-field solenoid is guided by our desire to optimize the output particle number for this highly divergent beam with an exponential energy spectrum. A future experimental test stand is proposed to do studies concerning the application as a new particle source.

INTRODUCTION

Ion acceleration from high-intensity, short-pulse laser irradiated thin metallic foils (figure 1) has attracted much attention during the past decade. The rear side emitted ion and, in particular, proton pulses contain large particle numbers ($> 10^{12}$) with energies up to 60 MeV [1] and are tightly confined in time ($< \text{ps}$) and space (source radius a few μm).

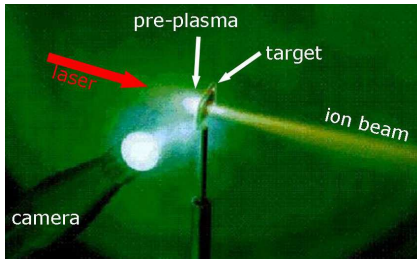


Figure 1: Photograph of the laser-ion-acceleration from a foil target at the LLNL NOVA Petawatt laser.

Relativistic electrons generated by the laser-plasma interaction penetrate through the target foil, escape on the rear side, and form an electron sheath resulting in an electric field of the order of TV/m on the rear surface. As the electric field points normally to the target surface, this rear-side accelerating mechanism is called *target normal sheath acceleration* [2]. Atoms at the rear surface, mostly protons present in impurities on the target surface, are field ionized and are accelerated normally from the surface into vacuum along the electric field lines. After the acceleration period, the proton beam experiences only thermal expansion. The space charge is neutralized due to comoving electrons.

For a better understanding of the acceleration mechanism and for controlling the beams it is crucial to have detailed information about the proton beam parameters such as source size, divergence, transverse emittance, and the spatial and energy resolved proton distribution. Measurements with radiochromic films (RCF) and micro-structured gold foils, called *RCF imaging spectroscopy* [3] and *Thomson parabola* analysis [4], quantify these properties. The spatial and energy resolved proton distribution and the energy dependent envelope-divergence for an example proton beam are shown in figure 2. The source size on the

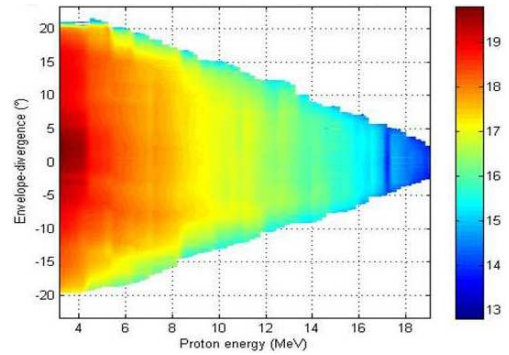


Figure 2: Proton beam parameter of a Trident laser shot, LANL. Logarithmic color scale in units of protons per $200 \text{ keV} \times \text{mm}^2$.

target rear side is decreasing for increasing proton energy, from $70 \mu\text{m}$ (6 eV) to $20 \mu\text{m}$ (14 MeV). The transverse emittance ϵ of the proton beam can be calculated from an ellipse fit in phase space or via the RMS emittance. For laser-accelerated proton beams, the relation $\epsilon_{\text{ellipse}} = 4 \times \epsilon_{\text{rms}}$ applicable for uniform beams matches pretty well. ϵ_{rms} also decreases for increasing proton energy, from 0.136 mm-mrad (6 MeV) to 0.028 mm-mrad (14 MeV).

The generation of these high-current beams is a promising new area of research and has motivated the development of applications such as tabletop proton sources or pre-accelerators. Requirements for an injector are controllability, reproducibility and a narrow (quasi-monoenergetic) energy. However, the source provides a divergent beam with an exponential energy spectrum that exhibits a sharp cut-off at its maximum energy. The laser and plasma physics group of the Technische Universität Darmstadt (TUD), in collaboration with the GSI Helmholtzzentrum für Schwerionenforschung (GSI), the Lawrence Berkeley National

* f.nuernberg@gsi.de

Laboratory (LBNL) and the Lawrence Livermore National Laboratory (LLNL), is studying possibilities for transport and RF capture in conventional accelerator structures.

EXPERIMENTS

Permanent magnet miniature quadrupoles

The first experiment carried out at the Z-Petawatt laser system, Sandia National Laboratories (NM, USA), demonstrates the transporting and focusing of laser-accelerated 14 MeV protons by permanent magnet miniature quadrupole lenses providing field gradients of up to 500 T/m [5]. The approach is highly reproducible and predictable, leading to a focal spot of $(286 \times 173) \mu\text{m}^2$ full width at half maximum 50 cm behind the source. The experimental setup is shown in figure 3. Due to the quadrupole arrangement and small aperture, the transmission of 14 MeV protons was limited to 0.1%, which is too low for further applications.

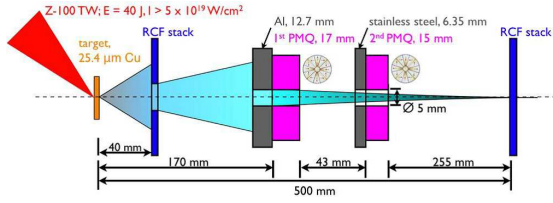


Figure 3: Setup of the proton beam transport and focusing experiment with 2 permanent magnet miniature quadrupoles at Z-Petawatt, Sandia National Laboratories.

Pulsed high-field solenoid

The aim for the following experiment at the Phelix laser system, GSI Darmstadt (Germany), was to enhance the transmission by increasing the magnet aperture. Therefore an available, pulsed solenoid has been modified to conform to the experiment. The last design of the solenoid mounting (figure 4) overcame the fracture limit and a magnetic field strength of 15 T could be achieved. The 72 mm

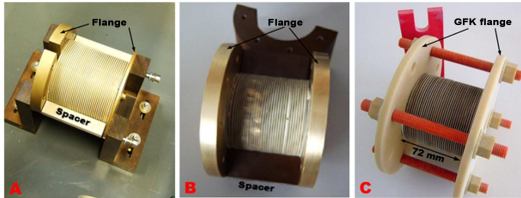


Figure 4: Evolution of the pulsed solenoid mounting at GSI to achieve maximum mechanical stability, from A to C.

long solenoid with an aperture of 44 mm consists of 33 brass windings. Due to interactions between the solenoid and the emerging plasma the final operating point was at 8 kV/19 kA resulting in a pulsed magnetic field of 8.6 T. For this magnetic flux density, simulations show a beam

collimation for a proton energy of 2.5 MeV. The original field of 15 T would lead to a collimation of 10 MeV protons.

The Phelix CPA laser system at GSI delivered 108 J on target, focused by a copper parabolic mirror to a beam spot of $16 \mu\text{m}$ (full width at half maximum). With a pulse duration around 700 fs, the intensity on the target foil ($10 \mu\text{m}$ Au) was $I > 3 \times 10^{19} \text{ W/cm}^2$. A picture of the experimental setup is shown in figure 5.

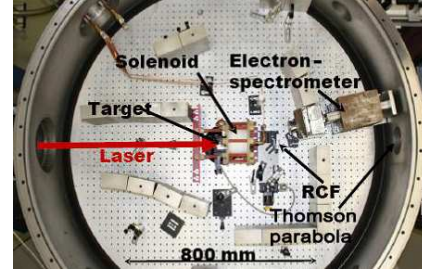


Figure 5: Target chamber setup for the pulsed solenoid experiment at the Phelix laser system.

RCFs in stack configuration enable energy resolved measurements of the beam profile. Each film can be attributed to a particular proton energy $\pm 0.5 \text{ MeV}$. Figure 6 shows the comparison of two RCFs during a shot without (top) and with solenoid field (bottom). The RCF stack was positioned 241 mm behind the target and the layer was $(5 \times 5) \text{ cm}^2$. Due to the high envelope-divergence, it was not possible to catch the full beam in the film (see fig. 6 top). Figure 6 bottom shows the proton beam profiles after modulation through the solenoid field. Not only was the flux increased, the full width at half maximum of the imprinted proton beam was smaller than the solenoid aperture. As the simulations predicted, protons around an energy of 2.5 MeV were collimated. The feature in the second film originated from the electron interaction (see CST simulations). However, further analysis is required to quantify the results.

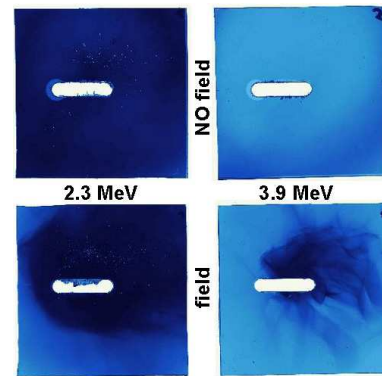


Figure 6: RCF comparison of proton beam energies without (top) and with (bottom) solenoid field. The slit in the films is for the line of sight of the spectrometers.

SIMULATIONS

Trace3D

Trace3D [6] is a well-known simulation code in accelerator physics used to calculate the beam envelope of a pulsed particle beam in a transport system consisting of different accelerator elements. Because Trace3d includes only linear effects in the solenoid, the envelope results were used as initial parameters for the CST simulations. Figure 7 shows the collimating and focusing energy of the primary setup with a magnet field strength of 15 T.

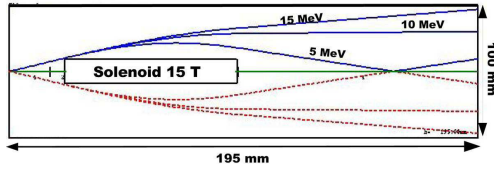


Figure 7: Trace3D simulation: vertical (red) and horizontal (blue) beam envelope.

CST Particle Studio

The simulation code CST Particle Studio enables designing accelerator elements and calculating their electromagnetic fields. Additionally, the trajectories of charged particles in these fields can be calculated. The Particle-In-Cell-Solver is also able to include Coulomb forces between particles. In figure 8 the effect of the co-moving electrons is included, but the particles are not plotted. The gyroradius of the electrons is much smaller than for protons, because of the lower electron energy (< 4 keV). Due to the high electron density, protons are attracted close to the beam axis.

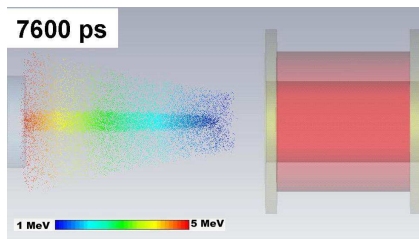


Figure 8: CST simulation: proton beam distribution behind the solenoid at $t = 7600$ ps and a magnetic field strength of 8.6 T (including Coulomb forces). The beam comes from the right image border and goes to the RCF detector on the left hand side.

Warp simulation code

The Warp suite of simulation codes [8] is used to improve these results. Input properties like arbitrary particle distributions, variable adjustment of all beam parameters, electrostatic self-fields and arbitrary applied fields make more detailed conclusion concerning beam behavior

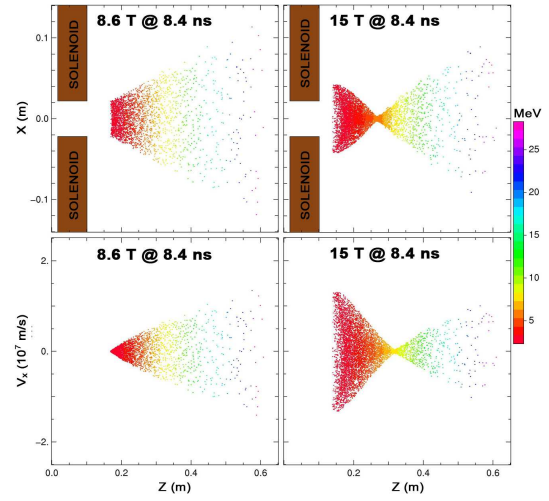


Figure 9: Warp simulations: (top) transverse deflection X and (bottom) transverse proton velocity V_x versus beam propagation direction Z for two different magnetic field strengths 8.6 T and 15 T at the time 8.23 ns. Injected proton energies: (2.3-28.7) MeV.

possible. Figure 9 shows the comparison of two simulations with different magnetic field strengths: 8.6 T (experiment) and 15 T (Trace3D simulation). The proton energies for collimation are 2.5 MeV (8.6 T) and 10 MeV (15 T). Further investigations are necessary, because the electrons and the electrostatic self-fields are not included yet.

OUTLOOK

The first experiments and also the results of the simulations point out several challenges to be worked out during the development of the test stand. Higher magnetic fields would be desirable to increase the proton energy for collimating. A compromise has to be found between the proton beam efficiency and the solenoid limits, such as the fracture limit of the solenoid mounting and the interaction of the solenoid and the plasma (flashover). The chromatic and spherical aberration of the solenoid makes the optimization difficult, too. Finally, the transverse emittance growth should not be too large. Nevertheless, these first results are promising, and the next experiments are scheduled.

REFERENCES

- [1] R. Snively *et al.*, Phys. Rev. Lett. **85**, 2945 (2000).
- [2] S. Wilks *et al.*, Phys. Plasmas **8**, 542 (2001).
- [3] F. Nürnberg *et al.*, Rev. Sci. Instrum. **80**, 033301 (2009).
- [4] K. Harres *et al.*, Rev. Sci. Instrum. **79**, 093306 (2008)
- [5] M. Schollmeier *et al.*, Phys. Rev. Lett. **101**, 55004 (2008).
- [6] Trace3D, <http://laacg1.lanl.gov/laacg/services>, 1997.
- [7] CST Studio Suite. <http://www.cst.de>, 2008.
- [8] D.P. Grote *et al.*, AIP Conference Proceedings, Volume **749**, Issue 1, pp. 55-58 (2005).

Rtgr ctgf "d{ 'NNP N'vpf gt'EqpvtcevF G/CE74/29PC495660'